New European wind atlas offshore

Karagali, Ioanna; Hahmann, Andrea N.; Badger, Merete; Hasager, Charlotte Bay; Mann, Jakob

Published in:
Journal of Physics: Conference Series

Link to article, DOI:
10.1088/1742-6596/1037/5/052007

Publication date:
2018

Document Version
Publisher's PDF, also known as Version of record

New European wind atlas offshore

New European wind atlas offshore

Ioanna Karagali, Andrea N Hahmann, Merete Badger, Charlotte Hasager and Jakob Mann

Frederiksborgvej 399, Building 125, Risø Campus, DK-4000, Roskilde, Denmark

E-mail: ioka@dtu.dk, ahah@dtu.dk, mebc@dtu.dk, cbha@dtu.dk, jmsq@dtu.dk

Abstract. The New European Wind Atlas (NEWA) is a joint research effort from eight European countries, co-funded under the ERANET Plus Program. The project's final aim is the creation and publication of an state-of-the-art electronic European wind atlas. An offshore wind atlas extending 100 km from the European coasts is foreseen within the project, based on mesoscale modelling and various observational datasets. Satellite wind retrievals from scatterometers and Synthetic Aperture Radar (SAR) instruments are used to validate offshore modelled wind fields and to identify the optimal model configuration. The aim is to present the initial outputs from the offshore wind atlas produced by the Weather and Research Forecasting (WRF) model, still in pre-operational phase, the METOP-A/B Advanced Scatterometer (ASCAT) and SAR derived winds. Different experiments were established to evaluate the model sensitivity for the various domains covered by the NEWA offshore atlas. ASCAT winds are used to assess the performance of the WRF-derived offshore atlas. In addition, ASCAT and SAR winds were used to create an offshore atlases, where various spatial wind characteristics, such as channelling and lee effects from complex coastal topographical features, are visualised.

1. Introduction

The aim of the New European Wind Atlas (NEWA) project is the creation and publication of a European wind atlas of unprecedented accuracy [28, 29]. Downscaling methodologies combining models of large-scale atmospheric flow to local flow at any potential wind turbine site [31] will be developed while measurement campaigns to validate such methodologies have been conducted. A popular description of the entire project is available in [2]. The NEWA project will provide a unified high-resolution and freely available data-set of wind resource and siting parameters in Europe. Wind statistics will cover onshore Europe and 100 km offshore over the European Seas, based on at least 10 years of mesoscale simulations. Mesoscale model simulations are used to calculate the wind resource with the implementation of the Weather Research and Forecasting (WRF) model [33].

Offshore wind resources over the European waters are of interest due to the increasing trend of wind farm installation in coastal areas, and recently further offshore (e.g. Hywind, [32]). Traditionally, measurements from meteorological masts are used for resource assessment, but installation and maintenance costs are extremely high while the spatial representativeness is limited. Atmospheric models can provide alternatives to account for better temporal and spatial resolution compared to *in-situ* measurements, although they suffer from lack of validation and subjectivity due to the model setup. The strength of the use of satellite wind fields to support offshore wind energy, lies in the capability to monitor large spatial domains over extensive

periods of time although the sampling frequency achieved from satellite wind retrievals can be considered poor compared to the sampling frequencies of typical *in-situ* sensors, i.e. 10 minute averages, or numerical models, i.e. hourly. Satellite observations of the wind over the ocean surface can prove valuable as indicators of the resource distribution and provide information about the areas where high-resolution mesoscale model experiments can be performed.

Wind speed at 10 m above the ocean surface is routinely retrieved from space-borne radars, i.e. Synthetic Aperture Radars (SAR) and scatterometers. These radar instruments are sensitive to cm-scale waves generated at the sea surface due to the instantaneous wind stress. The radar pulses are scattered from the ocean surface back to the instruments and the amount of back-scattered signal per unit area, i.e. the normalised radar cross section (NRCS), depends on the size and geometry of roughness elements on the scale of the radar wavelength at the Earth surface. In the case of a smooth surface, the returned NRCS is low due to reflection of the radar pulse away from the instrument. Roughness elements, generated by the surface wind stress as the wind over the ocean increases, increase the signal back-scattered to the instrument. The empirical relationships used for the retrieval of wind speed and direction, i.e. the Geophysical Model Functions (GMFs), are derived from the relation of the NRCS, the wind speed and direction at 10 m and the radar viewing geometry. GMFs are traditionally sensor or mission specific, and so far have been derived using the Equivalent Neutral Wind (ENW) notation [23] – the wind at 10 m assuming neutral atmospheric stratification. Due to multiple looks over the same area, scatterometers can retrieve the wind speed and direction but their spatial resolution is coarser than SAR winds [18]. The single look mode of SAR requires the *a priori* knowledge of wind direction to retrieve the wind speed. Global atmospheric models can provide wind directions at spatial scales comparable to that of SAR, and as such can be utilised for operational SAR wind retrievals.

SAR wind retrievals have been used to identify and study wind farm wakes offshore, e.g. in [11]. Wind resource assessment from Earth Observation ocean surface winds has been performed during the past decade, especially focusing on the northern European Seas. Winds from the Quick Scatterometer (QuikSCAT) and the European Remote-Sensing Satellite (ERS) SAR were used in [14] to perform an analysis of the wind resources in the North Sea, highlighting the applicability of SAR for local-scale and that of QuikSCAT for basin-scale studies. The amount of required ocean wind field retrievals to achieve accurate resource statistics was investigated in [14]. The full QuikSCAT archive was used in [15, 19, 21] to perform validation, resource assessment and long-term characterisation of the surface winds, especially their spatial variability compared to modelled wind fields. The full QuikSCAT and part of the Advanced Scatterometer (ASCAT) archive were used in [10], for validation with *in-situ* stations and to demonstrate the potential for the combined use of scatterometer observations from different platforms. Wind retrievals from the Environmental Satellite (Envisat) Advanced SAR (ASAR) have been used to perform wind resource estimations for various regions including Iceland [12], China [3], the Great Lakes [7], and the Baltic Sea [13] amongst others.

The advantages of satellite ocean surface winds over modelled winds due to the higher effective spatial resolution of the former, have been demonstrated in [22]. Studies have shown deficiencies in kinetic energy of modelled winds when compared to the ERS [4, 34] and QuikSCAT [30][33]. Recently, [18] examined the spectral characteristics of Envisat ASAR and QuikSCAT wind retrievals and showed the contribution of each sensor to describe spatial scales of different sizes. While the 10 m wind information can be resolved with satisfactory accuracy given the design characteristics of such space-borne sensors, atmospheric levels relevant for wind turbine operation are much higher and the extrapolation from 10 m depends on the atmospheric stability. Studies, e.g. [16] have shown that the marine boundary layer over the global ocean is, on average, slightly unstable. [1] performed an extrapolation of the mean wind from SAR at turbine relevant heights, using a long term stability corrected wind profile derived from mesoscale model

simulations.

In the present study, the 10-m wind information from SAR and scatterometers from 2002 to 2017 has been used to derive a mean wind "climate" over the European Seas. Since for wind turbine hub-heights offshore levels higher than 10 m are more relevant, extrapolation of the long-term mean winds to higher atmospheric levels was performed, using a 10-year long stability correction profile from the mesoscale model WRF [1]. In addition, comparisons between the satellite derived offshore winds and the WRF model outputs were used to assess the spatial variability of the mean wind speed at different heights and the impact of different WRF tuning options on the modelled outputs.

A description of the data and methods used is presented in Section 2, while the relevant results are shown in Section 3. Finally, discussions and the main conclusions are summarised in Section 4.

2. Data and Methods

2.1. Satellite data

The ASCAT and SAR wind retrievals are treated separately, thus two different long-term climatologies were produced. A summary of the products and specifications is found in Table 1. SAR wind retrievals are routinely performed at DTU Wind Energy, using a processing chain built around the SAR Ocean Products System (SAROPS) by the NOAA Center for Satellite Applications and Research (STAR), US National Ice Center and Johns Hopkins University, Applied Physics Laboratory [24]. The SAR wind retrievals are performed using the CMOD5.N GMF, thus are representative of the Equivalent Neutral Wind (ENW), at a 600 m resolution to eliminate effects of random noise and of surface inclination due to longer-period ocean waves. The derived SAR climatology has a 2 km resolution, while for ASCAT the original spatial grid of 12.5 km is maintained.

Table 1. List of space-borne sensors and products used.

Sensor	Type	Period	Band	Wind retrieval	Retrieval
ASCAT (MetOp-A)	Scatterometer	2007 - now	C	KNMI	speed, direction
ASCAT (MetOp-B)	Scatterometer	2012 - now	C	KNMI	speed, direction
ENVISAT ASAR	SAR	2002 - 2012	C	DTU Wind Energy	speed
Sentinel-1	SAR	2015 - now	C	DTU Wind Energy	speed

2.1.1. ASCAT The European Organisation for the Exploitation of Meteorological Satellites (EUMETSAT) operates a series of polar orbiting meteorological satellites (MetOp), two of which are already in orbit with the third one scheduled for launch in October 2018. ASCAT is the C-band scatterometer on board both MetOp-A and MetOp-B, measuring in two 500 km-wide swaths. The wind product used in the present study is the newly available 12.5 km Coastal Stress Equivalent Wind, obtained through the Copernicus Marine Environmental Monitoring Service (CMEMS, `http://marine.copernicus.eu/`, [5]).

2.1.2. Envisat The European Space Agency (ESA) platform Envisat was launched in 2002 and its data acquisition was terminated in April 2012. It carried, amongst other instruments, an Advanced Synthetic Aperture Radar (ASAR) operating in C-band with several different modes. The majority of Envisat ASAR scenes in this archive have been acquired in Wide Swath mode

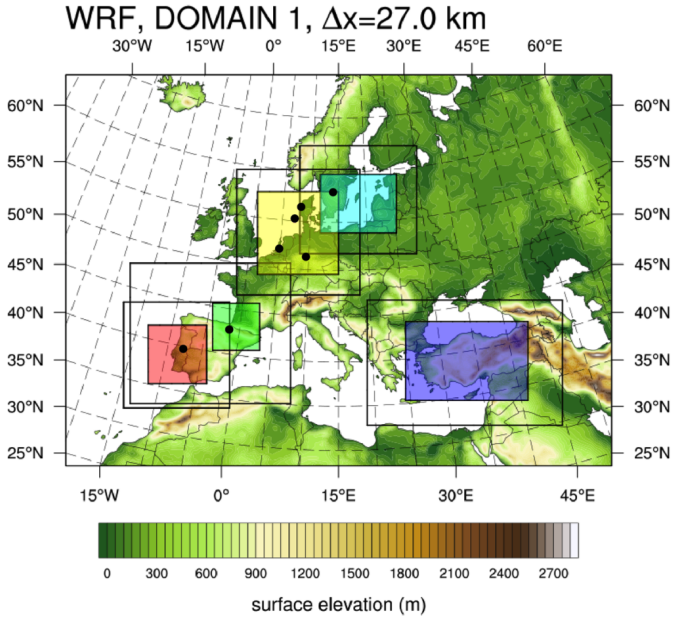

Figure 1. The WRF outer domain over Europe with the 5 nested, higher resolution domains shaded in different colours: NE (turquoise), NW (yellow), PE (red), SW (green) and SE (purple). The black dots represent sites of experimental measurement campaigns during the NEWA project.

(WSM) or Global Monitoring mode (GMM) with a swath width of 400 km and variable lengths. The Image mode (IM) and Alternating Polarisation mode (APP) are suitable for ocean wind retrieval over smaller areas due to their swath width of 100 km. This archive holds a limited collection of processed data based on these modes.

2.1.3. Sentinel-1 Another ESA mission, Sentinel-1 consists of two separate platforms, each with a C-band SAR (5.3 GHz) on board. Sentinel-1A was launched on 3 April 2014 and Sentinel-1B on 25 April 2016. Both sensors are currently operational.

2.2. Modelling

Mesoscale models cover a limited area and require lateral boundary conditions from a global reanalysis product, which uses data assimilation to produce the best possible representation of the state of the atmosphere every 3 or 6 hours at horizontal resolutions of several tens of kilometres. NEWA uses the Weather Research and Forecasting (WRF) mesoscale model [33]. Simulations were performed for the test year of 2015 using the method of [8] to determine some fundamental settings and strategies known to have a significant impact on the wind resource estimation. Two different simulations are used for the purposes of the present study, with a common daily initialisation at 00:00 GMT and a difference of the selected Planetary Boundary Layer (PBL) scheme, i.e. MYNN and YSU. These two simulations are be named as MYNL61S1 and YSUL61S1 and will be referred to using these code names for the remaining of the manuscript.

For these sensitivity simulations, five inner domains were established over Europe, with a resolution of 3 km, with an outer domain of 27 km, see Figure 2.2. The location of domains was chosen to cover different geographical regions of Europe and locations of high quality measurements or experiments carried out during the NEWA project. The North-West (NW) domain, on which this study focuses, covers the Kassel forested hill, the RUNE coastal and Østerild balconies experiments along with the series of three FINO offshore masts.

The global atmospheric reanalysis ERA Interim, with a resolution of 0.75° ×0.75°, from the European Centre for Medium Range Weather Forecasting (ECMWF) was used to obtain lateral boundary conditions [6]. The Optimal Interpolation Sea Surface Temperature (OISST), [30], at

0.25° ×0.25° from the National Oceanic & Atmospheric Administration (NOAA) including sea ice concentrations along with a lake product were used to assign water points. CORINE land surface data were used, while the surface roughness coefficient for each land cell was assumed constant over time.

2.3. Extrapolating surface winds

All available and valid observations from ASCAT and SAR were used to derive the mean wind at 10 m above the surface. In the case of ASCAT, grid cells with more than 500 observations were used to minimise the uncertainty of the derived results. This was not applied for the SAR retrievals, due to their inconsistent coverage.

The long-term stability correction is derived using 10 years of hourly WRF model outputs from the ENTSO-E project [25], using the method described in [1]. This long-term stability correction can be interpreted following [26] and was applied to the mean 10 m winds from ASCAT and SAR for extrapolation at various atmospheric levels, i.e. from 1 m up to 150 m with a resolution of 1 m.

3. Results

3.1. Satellite wind climatologies

The long term mean wind at 10 m above the ocean surface from ASCAT along with the number of used observations per grid cell is presented in Figure 2. The very high number of observations noted for the higher latitudes is an outcome of the polar orbiting nature of the MetOp platforms, where the frequent orbits combined with the wide swath result in a higher number of observations per day.

For the latitudes of interest, the number of available ASCAT observations ranges between 5000 and 7000 samples, which could be translated to 500 to 700 samples per year. The reduction of samples very close to the coast is related to quality controlling wind retrievals of increased proximity to the land, due to contamination in the radar backscatter. This contamination is related to the fundamentally different scattering properties of land compared to water, in the operational wavelengths of the ASCAT instrument.

The mean wind during the decade of available ASCAT retrievals shows distinct patterns around the European Seas. Higher mean winds are recorded in the North Sea and the North Atlantic compared to the Mediterranean, Baltic and Black Sea. Characteristic features such as the Mistral wind in the Gulf of Lyons and the Etesians in the Aegean Sea, appear as areas with increased mean winds in the Mediterranean Sea.

The corresponding long-term mean wind at 10 m from the combination of Sentinel-1 and ASAR retrievals, along with the number of observations per grid cell is presented in Figure 3. A significantly reduced, compared to ASCAT, pattern of data availability is visible, with maximum number of observations barely exceeding 1800. This is related to the lower overpass frequency of Envisat and Sentinel-1. The highest number of observations available is recorded for the North and Baltic Sea and the area around Brittany in France.

The magnitude of the mean wind speed from SAR is higher than ASCAT (Figure 3, right panel) over the period of SAR data, i.e. 2002-2017, with preliminary results indicating that the difference can reach up to $1.5\,\mathrm{m\,s^{-1}}$ for some areas. Deriving the friction velocity, u_*, from the two products using a logarithmic wind profile, indicated that differences were less than $0.08\,\mathrm{m\,s^{-1}}$ (not shown). Nonetheless, the spatial patterns are very similar to what is observed by ASCAT with the intense gradient of the mean wind with increasing trend from South to North Europe, topographic features causing particular wind patterns. Such results provide some assurance that the sample size required to capture wind characteristics is reached in both climatologies.

The long-term mean wind speed extrapolated at 100 m is presented in Figure 4, from ASCAT (left) and SAR (right). Higher values compared to the ones at 10 m are systematically

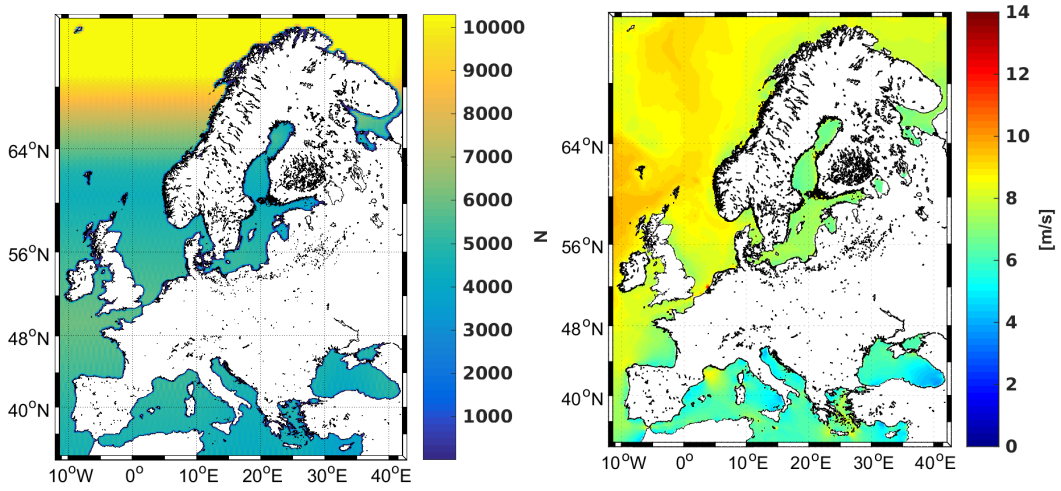

Figure 2. Number of available samples per grid cell from ASCAT (left) and mean wind speed at 10 m (right).

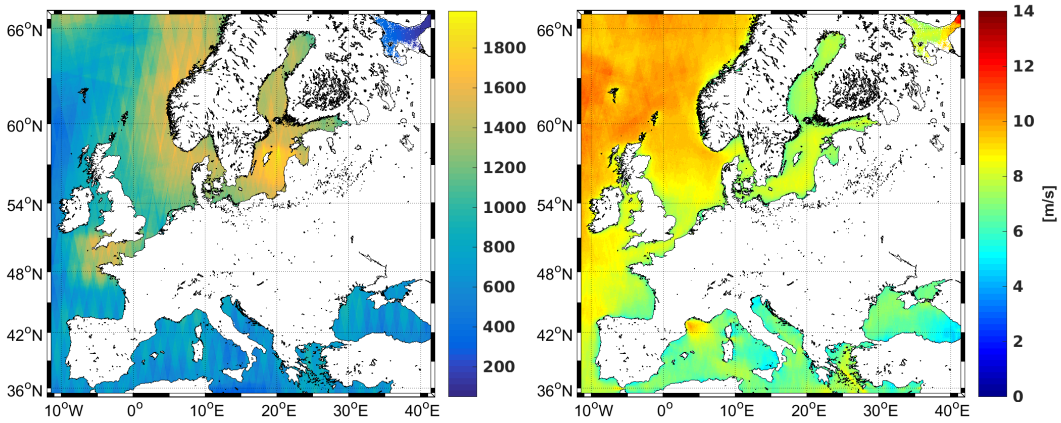

Figure 3. Number of available samples per grid cell from the combination of Envisat-ASAR and Sentinel-1 (left) and mean wind speed at 10 m (right).

observed. Noticeable differences between the two climatologies consist of an increased magnitude estimation from SAR compared to ASCAT by approximately $1.5\,\mathrm{m\,s^{-1}}$ at 100 m throughout the domain. This difference persists from the findings of the 10 m winds, although somewhat higher, $\sim 0.2\,\mathrm{m\,s^{-1}}$.

The systematic difference in the magnitude of the wind observed from ASCAT and SAR (Figure 4) can be associated to the Equivalent Neutral Wind (ENW) notation versus the Stress Equivalent Wind. SAR winds are ENW and in the case of dominant unstable conditions as the marine boundary layer is overall known to be, ENW are and overestimated version of the naturally occurring wind by approximately $0.5\,\mathrm{m\,s^{-1}}$, see [21] and references therein. Although similar differences between Sentinel-1 and ASCAT have been reported in [24], validation of the two products with *in situ* meteorological mast measurements is on going but outside the scope of the present study.

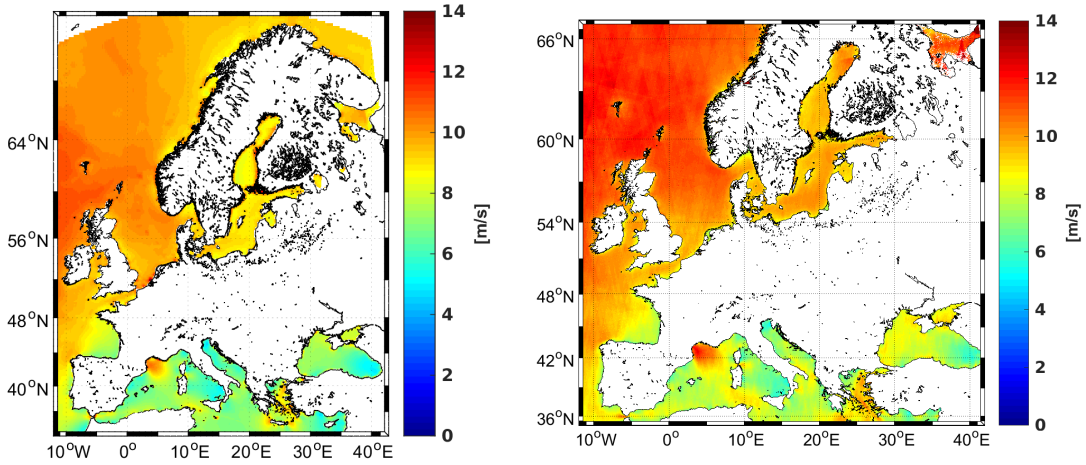

Figure 4. Mean wind speed at 100 m from ASCAT (left) and the combination of Envisat-ASAR and Sentinel-1 (right).

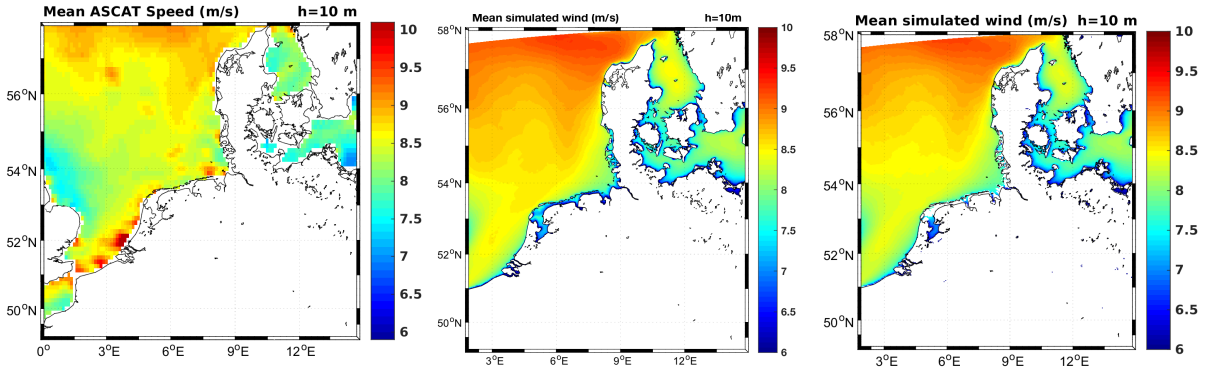

Figure 5. Mean wind speed at 10 m above the ocean surface from ASCAT (left) and WRF using the MYNN (middle) and YSU (right) PBL schemes, for 2015.

3.2. Satellite versus simulated winds

The mean wind speed over the west part of the North Europe domain, as defined within the NEWA project, for 2015 from ASCAT and the two versions of the WRF model are shown in Figure 5. The spatial variability in the WRF simulations is noticeably different, and reduced, compared to ASCAT. Slightly lower winds are observed by ASCAT compared to both WRF simulations, by 0.5 $\mathrm{m\,s^{-1}}$ on average. Exceptions are found in areas with intensively higher ASCAT winds, such as the areas offshore from the Netherlands and Bremen-haven. In these cases, ASCAT higher winds can be partially considered as artefacts due to i) the consistent presence of ships offshore Rotterdam port and ii) the high concentration of wind farms north of Bremen-haven. Both ships and wind turbines, considered as hard targets, can increase the signal back-scattered to the instrument and thus the derived wind speed magnitude. Existing studies, e.g. [1, 19, 27], comparing satellite winds with WRF model outputs have found lack of spatio-temporal variability in the model compared to the wind retrievals, while absolute magnitudes of differences depend also on the model set-up amongst others. Differences in the spatial patterns of the mean wind speed are also noted between the simulations, which have absolute magnitude differences of the mean wind speed up to 0.4 $\mathrm{m\,s^{-1}}$ amongst them.

The percentages of unstable conditions were derived from the surface-layer Monin-Obukov stability parameter, L, an output field from the simulations and are shown in the left panel of

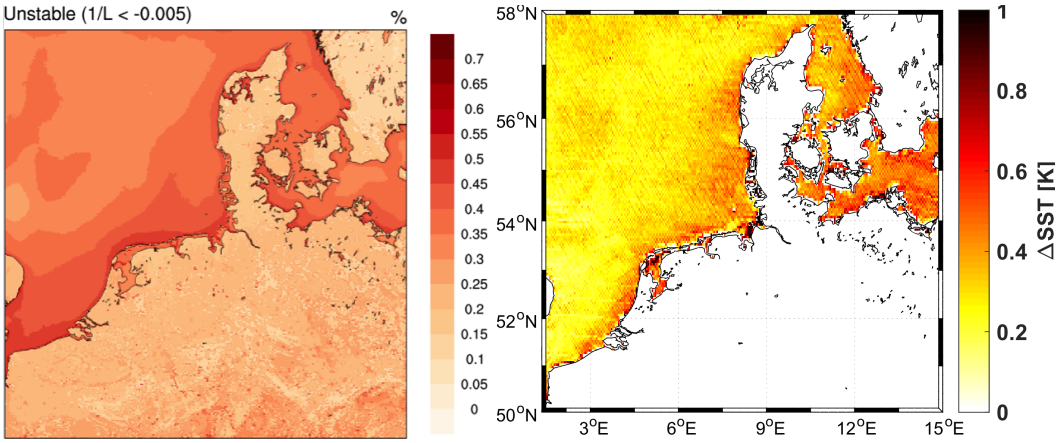

Figure 6. Fraction of unstable conditions over the North Sea during 2015 as simulated by WRF during the sensitivity experiments (left). Mean of the sea surface temperature maximum diurnal variability from 2006 to 2012 (right).

Figure 6. Over the water conditions are frequently unstable, especially closer to the coast lines and in particular off the shore of the Netherlands, Belgium and Germany. As mentioned before, equivalent neutral winds (ENW) from satellites will be higher than naturally occurring winds under unstable conditions.

Results (not shown here) indicated that atmospheric stability is an important parameter to explain the model sensitivity. To interpret the frequency of unstable conditions over the North Sea, findings from [20] are used. The right panel of Figure 6, adapted from [20], shows an estimate of the maximum diurnal variability signal of the sea surface temperature (SST). This signal was defined as the mean SST during a day (24 h) minus the foundation SST of that day, i.e. the SST under well mixed conditions or during night-time. This provided a daily mean diurnal warming estimate which was averaged monthly and Figure 6 shows the maximum of these values.

The spatial match of most frequently unstable conditions from WRF corresponds well to areas with highest amplitudes of the diurnal temperature cycle. This can be explained by the fact that large and sudden increases of the surface temperature occurring under clear sky and up to moderate wind conditions of $\sim 6\ \mathrm{m\,s^{-1}}$ [17], result in unstable conditions. This is a good indicator that a proper and accurate SST boundary condition should be used for the simulations.

Mean winds at 100 m were part of the WRF output simulations and have been computed for 2015. Figure 7 shows results from the two different WRF simulations, consisting of different PBL schemes (left and middle). The difference between the two simulations is shown in the right panel of Figure 7. It is found that for the domain of interest differences between the two WRF simulations, at 100 m, do not exceed $0.2\ \mathrm{m\,s^{-1}}$, with mostly higher mean wind speeds for the MYNL61S1 simulation. This is a positive outcome given that differences between the two simulations shown in Figure 5 are higher, up to $0.4\mathrm{m\,s^{-1}}$. Moreover, both simulations provide similar results to the 100 m extrapolated mean wind from the ASCAT and SAR winds (see Figure 4) in terms of the spatial variability. Nonetheless, magnitude differences do exist and are in the order of $1\mathrm{m\,s^{-1}}$ between WRF and ASCAT at 100 m, consistent throughout the domain of interest. Between SAR and WRF at 100 m apart from large parts of the domain with similar $1\mathrm{m\,s^{-1}}$ magnitude difference, a region the central North Sea basin showed differences in the order of $0.3\mathrm{m\,s^{-1}}$. Such comparisons should be taken with caution since the mean wind speed from WRF was derived only from the 2015 simulations, while the extrapolated satellite winds are representative of longer time-scales.

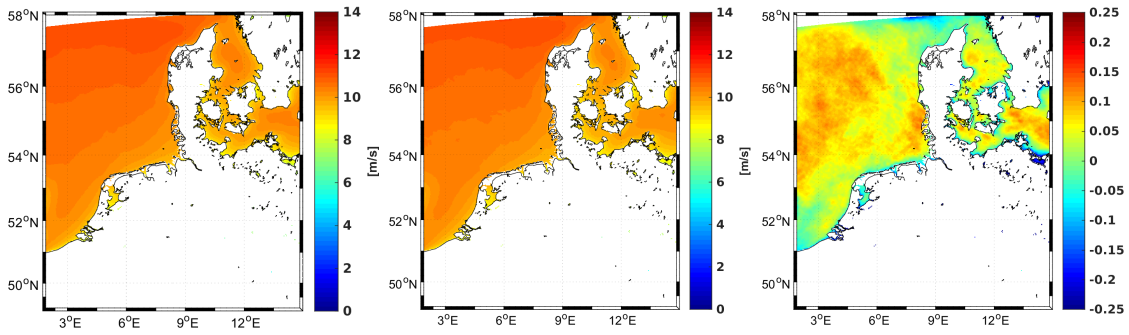

Figure 7. Mean wind speed at 100 m for 2015 from WRF using the MYNN (left) and YSU (middle) PBL schemes along with the difference between the two (right).

From results (not shown here) of the northern Europe domains, over the sea, the annual mean wind speeds of the MYNL61S1 simulation are only +0.1 $\mathrm{m\,s^{-1}}$ higher than those of the YSUL61S1, but are slightly negative in the southern Europe domains. The ratio of the hourly wind speed standard deviation is very close to one for the two PBL schemes, except for the winds over the coastal Mediterranean seas where the YSU scheme has larger variance than the MYNN scheme.

4. Conclusions

This study demonstrates the use of wind information over the ocean as derived by satellites during the last 16 years, to describe "long-term" features of the offshore wind conditions, within the framework of the New European Wind Atlas project. In addition, the satellite derived wind atlases were used for an initial comparison with wind fields simulated using WRF for 2015, during the sensitivity test phase of the project. Although the temporal availability of satellite wind retrievals is reduced compared to *in-situ* measurements and model simulations, mean wind speeds over the entire period of satellite data availability revealed persistent features, common in both the ASCAT and SAR datasets. The mean wind speed at 10 m was found to be consistently higher from SAR, by up to 1.5$\mathrm{m\,s^{-1}}$, and attributable to the different geophysical model functions applied for the wind retrieval and the different sensor characteristics. Efforts to validate the different wind products, and particularly the new ASCAT product are ongoing. Satellite winds were extrapolated to 100 m using a long-term stability correction derived from WRF simulations and these results revealed increased mean wind speeds over the entire domain of interest, while maintaining spatial features connected with topography and persistent wind patterns, e.g. the Mistral wind and the Etesians. When compared to the WRF model simulations for 2015, ASCAT mean wind speeds showed higher spatial variability, although wind speed magnitude differences were on average up to 0.3 $\mathrm{m\,s^{-1}}$, with exceptions being associated to artefacts in the ASCAT mean wind speed. WRF mean wind speeds simulated using different PBL schemes showed differences of 0.4$\mathrm{m\,s^{-1}}$ at 10 m which decreased to 0.25$\mathrm{m\,s^{-1}}$ at 100 m. Furthermore, an increased sensitivity to the atmospheric stability was observed and very frequent unstable conditions occurred in the North Sea domain. Sea surface temperature fields were used to interpret such frequently unstable conditions, with a good spatial agreement between relatively large day-time increase of the SST and the frequency of unstable WRF simulations. Finally, the mean wind speed simulated from WRF at 100 m for 2015 was found to be in good spatial agreement with the satellite extrapolated mean wind speed from ASCAT and SAR, although with a relatively persistent 1$\mathrm{m\,s^{-1}}$ magnitude difference. This study has demonstrated the use of satellite wind retrievals over the ocean to derive long-term wind characteristics at 10 m that can, by applying a long-term stability correction, be extrapolated to higher atmospheric levels

while maintaining original attributes, e.g spatial variability and topographic features. Moreover, this study has shown that such satellite derived winds can be useful for evaluating sensitivities from mesocale model simulations.

Acknowledgments
EUMETSAT, KNMI & the Copernicus CMEMS service for ASCAT data & SEVIRI SST data used in Figure 6. ESA for ENVISAT ASAR & Sentinel-1 data. The Global Wind Atlas project for hosting the online version of the satellite wind climatologies at `http://science.globalwindatlas.info/science.html`

References

[1] Badger M, Peña A, Hahmann A N, Mouche A and Hasager C B 2016 *J Appl Meteorol Clim* **55** 975.
[2] Calamia J 2017 *New Sci* **234 (3126)** 31–3.
[3] Chang R, Zhu R, Badger M, Hasager CB, Zhou R, Ye D and Zhang X 2014 *Energies* **7 (5)** 3339–54.
[4] Chin T M, Milliff R F and Large W G 1998 *J Atmos Ocean Tech* **15** 741–63
[5] de Kloe J, Stoffelen A and Verhoef A 2017 *IEEE J Sel Topics Appl Earth Observ in Remote Sens* **10 (5)** 2340–7
[6] Dee D P, Uppala S M, Simmons A J, Berrisford P, Poli P, Kobayashi S, Andrae U, Balmaseda M A, Balsamo G, Bauer P, Bechtold et al. 2011 *Q J R Meteorol Soc* **137 (656)** 553–97.
[7] Doubrawa P, Barthelmie R J, Pryor S C, Hasager C B, Badger M and Karagali I 2015 *Remote Sens Environ* **168** 349
[8] Hahmann A N, Vincent C L, Pea A, Lange J and Hasager C B 2015 *Int J Climatol* **35** 3422–39.
[9] Hasager C B, Nygaard N G, Volker P, Karagali I, Andersen S J and Badger J 2017 *Energies* **10 (3)**
[10] Hasager C B, Mouche A, Badger M, Bingöl F, Karagali I, Driesenaar T, Stoffelen A, Peña A and Longépé N 2015 *Remote Sens Environ*, **156**, 247
[11] Hasager C B, Vincent P, Badger J, Badger M, Di Bella A, Pena Diaz A, et al 2015 *Energies* **8 (6)** 5413–39.
[12] Hasager CB, Badger M, Nawri N, Rugaard Furevik B, Petersen GN, Bjrnsson H and Clausen N-E 2015 *IEEE J Sel Topics Appl Earth Observ in Remote Sens* **8 (12)** 5541–52.
[13] Hasager CB, Badger M, Pea A, Larsén XG and Bingöl F 2011 *Remote Sens-Basel* **3 (1)** 117–144.
[14] Hasager C B, Peña A, Christiansen M B, Astrup P, Nielsen M, Monaldo F, Thompson D and Nielsen P 2008 *IEEE J Sel Topics Appl Earth Observ in Remote Sens* **1 (1)** 67–79.
[15] Horstmann J, Koch W and Lehner S 2004 *Ocean Dyn* **54** 570–6.
[16] Kara A B, Wallcraft A J and Bourassa M A 2008 *J Geophys Res* **113** C04009.
[17] Karagali I, Høyer J L and Hasager C B 2012 *Remote Sens Environ* **121** 159–70.
[18] Karagali I, Larsén X G, Badger M and Hasager C B 2013 *Remote Sens-Basel* **5 (11)** 6069
[19] Karagali I, Badger M, Hahmann A, Peña A, Hasager C B and Sempreviva A M 2013 *Renew Energ* **57** 200
[20] Karagali I and Høyer J L 2014 *Ocean Sci* **10 (1)** 1–14.
[21] Karagali I, Peña A, Badger M and Hasager C B 2014 *Wind Energy* **17 (1)** 123
[22] Larsén XG, Ott S, Badger J, Hahmann A and J Mann 2012 *J Appl Meteorol Clim* **51** 521–53.
[23] Liu WT, and Tang W 1996 National Aeronautics and Space Administration, Jet Propulsion Laboratory, California Institute of Technology, National Technical Information Service.
[24] Monaldo F, Jackson C, Li X and Pichel W G 2015 *IEEE J Sel Topics Appl Earth Observ in Remote Sens* **9 (6)** 2638–42.
[25] Nuño Martinez E, Maule P, Hahmann A N, Cutululis N A, Sørensen P E and Karagali I 2018 *Renew Energ* **118** 425–36
[26] Peña A and Hahmann A N 2012 *Wind Energy* **15** 717–31.
[27] Peña Diaz A, Hahmann A N, Hasager C B, Bingöl F, Karagali I, Badger J et al. 2011 *Roskilde: Danmarks Tekniske Universitet, Ris Nationallaboratoriet for Bredygtig Energi* 66 p.
[28] Petersen E L, Troen I, Jørgensen H E and Mann J 2013 *Environ Res Lett* **8 (1)**
[29] Petersen E L 2017 *J Renew Sustain Ener* **9 (5)**
[30] Reynolds R W, Rayner N A, Smith T M, Stokes D C and Wang W Q 2002 *J Climate* **15 (13)** 1609–25.
[31] Sanz R J, Chavez Arroyo R A, Moriarty P, Churchfield M, Kosović B, Réthoré P-E, Hansen K S, Hahmann A, Mirocha J D and Rife D 2017 *WIRES Energy Environ* **6 (2)**
[32] Skaare B, Nielsen F G, Hanson T D, Yttervik R, Havmøller and Rekdal A 2015 *Wind Energy* **18 (6)** 1105–22.
[33] Skamarock W C, Klemp J B, Dudhia J, Gill D O, Barker D M, *et al.* 2008 *Tech. Rep.* NCAR/TN-475+STR National Center for Atmospheric Research
[34] Wikle C K, Milliff R E and Large W G 1999 *J Atmos Sci* **56** 2222-31.